Relative Tropospheric Photolysis Rates of HCHO, $H^{13}CHO$, $HCH^{18}O$, and DCDO Measured at the European Photoreactor Facility

Karen L. Feilberg,*,† Barbara D'Anna,‡ Matthew S. Johnson,† and Claus J. Nielsen‡

Department of Chemistry, University of Copenhagen, Universitetsparken 5 DK-2100 Copenhagen OE, Denmark, and Department of Chemistry, University of Oslo, Pb. 1033-Blindern 0315 Oslo, Norway

Received: March 16, 2005; In Final Form: June 13, 2005

The relative photolysis rates of HCHO, $H^{13}CHO$, $HCH^{18}O$, and DCDO were studied in pseudo-natural tropospheric conditions in July 2003 at the European Photoreactor Facility (EUPHORE) in Valencia, Spain. The photolytic decay of HCHO, $H^{13}CHO$, and $HCH^{18}O$ is measured relative to DCDO by long path FT-IR detection during the course of about 3 h of sunlight. The relative photolysis rates obtained are as follows: $J_{H^{13}CHO}/J_{HCHO} = 0.894 \pm 0.006$, $J_{HCH^{18}O}/J_{HCHO} = 0.911 \pm 0.011$, and $J_{DCDO}/J_{HCHO} = 0.597 \pm 0.001$. The errors represent 1σ and do not include possible systematic errors. The atmospheric implications of the large isotope effects in the photolysis of formaldehyde are discussed.

1. Introduction

Formaldehyde (HCHO) is the most abundant carbonyl compound in the atmosphere. It is present in remote, nonpolluted air with an average mixing ratio of 10−100 ppt, as well as in polluted air where it can reach 1−20 ppb.[1] It is an important intermediate species in the photochemical oxidation of methane and nonmethane hydrocarbons throughout the atmosphere. The major sources of formaldehyde are the photochemical oxidation of hydrocarbons and fossil fuel combustion, with biomass burning and microbiological processes being minor sources. Methane oxidation is the largest source of HCHO globally; however, in rural and forested areas oxidation of nonmethane hydrocarbons, such as isoprene, can be the dominant source.[2] In industrial areas, direct emission can contribute significantly to HCHO concentrations. The photochemical decomposition of HCHO provides about 40% of the atmospheric CO source and half of the H_2 source, and is a significant source of HO_x radicals in the atmosphere. Recently, measurements of HCHO in the upper troposphere and marine boundary layer have shown that the concentrations may be higher than current models predict, and that there may be unknown sources of HCHO in these areas.[3,4]

The main removal pathways for formaldehyde in the troposphere are photolysis, reaction with radicals, and deposition.[2,5] During the day, photolysis and reaction with photochemically produced radicals remove about equal amounts of formaldehyde.[6] OH is by far the most important radical and the global atmospheric lifetime of HCHO with respect to OH is about 24 h. In the marine boundary layer Cl radicals can dominate HCHO removal although the average global lifetime with respect to Cl is about two months.[7,8] At night, the reaction with the nitrate radical can contribute to HCHO loss.[9] During ground level ozone depletion events in the arctic marine boundary layer HCHO has been identified as an important sink for Br radicals. In addition the $Br + H_2CO$ reaction is likely to be an important mechanism converting stratospheric BrOx to HBr, as Br does not react with CH_4.[10,11] Formaldehyde is also removed by photolysis, and by reaction with $O(^1D)$ in the stratosphere.

The photolysis of formaldehyde can proceed via two pathways at atmospherically relevant wavelengths:

$$HCHO + h\nu \rightarrow H + HCO \qquad (\lambda \le 330\ \text{nm}) \qquad (1a)$$

$$HCHO + h\nu \rightarrow H_2 + CO \qquad (\lambda \le 361\ \text{nm}) \qquad (1b)$$

The quantum yield of the two pathways depends on wavelength, and thus varies throughout the troposphere.[12] Under average tropospheric conditions, most HCHO is photolyzed to H_2 and CO (reaction 1b), while a significant fraction is photolyzed to radicals (reaction 1a).[5,13] The photolysis of formaldehyde occurs by excitation from the ground singlet state of the molecule to the first excited singlet state with subsequent dissociation via both channels 1a and 1b. From the first excited state, a spin-forbidden transition to the first excited triplet state can take place, leading to dissociation via channel 1a.[14] The radical channel 1a is an important source of HO_x in the upper atmosphere where there is little water vapor, and the molecular channel is the only significant photochemical source of atmospheric H_2, producing half of all tropospheric molecular hydrogen.

The sources and sinks of formaldehyde in the atmosphere are not sufficiently characterized and the roles of transport, heterogeneous chemistry, and halogen reactions are still uncertain.[15] Analysis of the stable isotope composition of atmospheric species is a promising method for tracking sources and sinks of atmospheric gaseous species.[16] Different sources have different distinguishable isotopic signatures and the removal processes are likewise associated with distinct fractionations for stable isotopes. In the case of formaldehyde, characterization of the isotope effects in the loss processes is an important step in tracing carbon, hydrogen, and oxygen isotopes in the processes throughout the methane oxidation mechanism.

The reactions of HCHO with OH, Cl, Br, $O(^1D)$, and NO_3 are all associated with kinetic isotope effects (KIEs) which can distinguish the different reactions.[17,18] In most cases, the heavy isotope reacts more slowly with the radical species than the most

---

* Address correspondence to this author.

† University of Copenhagen.

‡ University of Oslo.

10.1021/jp0513723 CCC: $30.25

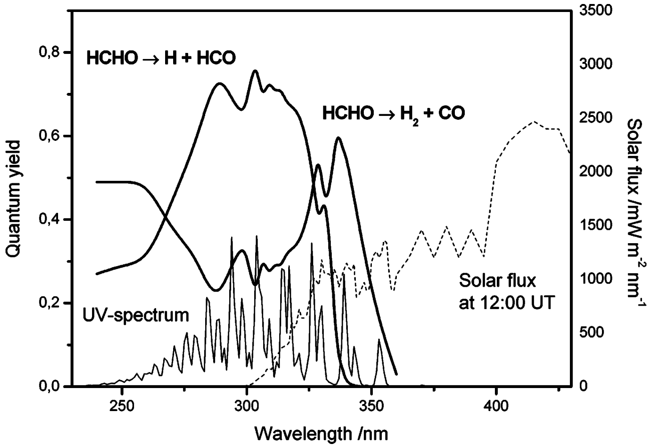

Figure 1. Solar flux measured during a typical experiment in the EUPHORE chamber (mW m^{-2} nm^{-1}), UV spectrum, and the quantum yields of photolysis of formaldehyde at atmospheric pressure. The UV spectrum and quantum yield data for the two photolysis processes are from the JPL Chemical Kinetics and Photochemical Database.[34]

abundant isotope leading to an enrichment of heavy isotopomers of HCHO. We have previously shown that the formaldehyde reactions with OH, Br, Cl, and NO_3 radicals exhibit large hydrogen KIEs for DCDO ranging from 300‰ for Cl to 7500‰ for Br, while the ^{13}C KIEs are of the order of −48‰ (for the OH reaction) to 130‰.[18−21] Likewise the UV spectrum of formaldehyde is shifted by isotopic substitution leading to an isotope effect in the photolysis.[22−27] Isotope effects in atmospheric photolysis has been shown to be a powerful tool for tracing other atmospheric trace gases, such as OCS, N_2O, SO_2, and CO_2.[28−31] It has been suggested that isotope effects in the photolysis of SO_2 early in the planet's history can help to identify the point in time when the oxygen-containing atmosphere emerged.[32] The present work extends the studies of reaction kinetic isotope effects of formaldehyde by addressing the isotope effects in the photolysis processes.

2. Experimental Section

The experiments described in this work were carried out in the period July 15−23, 2003 at the European Photoreactor Facility (EUPHORE) in Valencia, Spain (longitude −0.5, latitude 39.5). EUPHORE consists of two dome-shaped chambers (A and B) made of fluorinated ethene−propene (FEP) each with a volume of about 200 m^3. The FEP foil (thickness of 0.127 mm) has a transmission of more than 75% of the solar radiation in the wavelength range between 290 and 550 nm. The large volume of the chambers minimizes the effects of wall reactions, thus resembling the free troposphere as closely as possible. An example of the solar flux measured at EUPHORE is shown in Figure 1. Unlike the typical laboratory smog chamber, a certain amount of leakage through the FEP is unavoidable and this has to be corrected for in the data analysis. Also, ambient air diffuses in, and a small amount of NO_x will always be present in the chamber. The chambers are protected by a pneumatically controlled metal shielding when not in use.

The two chambers are equipped with state of the art instrumentation for many different types of analysis and these are operated from a laboratory situated underneath the chambers. A detailed description of the EUPHORE facility is given by Becker;[33] in the following we will focus on the system for in situ optical measurements of gaseous species in chamber A. The chamber is equipped with a White-type optical system coupled to an FTIR spectrometer (NICOLET Magna 550) with a liquid N_2 cooled MCT detector. The total optical path length in chamber A is 653.5 m, and the IR spectra were used to monitor the concentrations of reagents in the chamber. In addition, NO_x, CO, and O_3 were measured with separate monitors. Chamber A is kept at a constant, slightly above ambient pressure to obtain as constant a leak rate as possible and to minimize diffusion of ambient air into the chamber. A typical experiment starts at 06:00 UT when reagents are added to the chamber. The metal shield of the chamber is then opened at 07:00 UT after a few spectra of the dark chamber have been recorded and the reagents are considered to be well-mixed. Depending on the photolysis rates of the reagents, the experiment lasts 3−6 h after which the chamber is closed and flushed overnight with scrubbed air.

To study the relative photolysis rates of formaldehyde isotopomers, HCHO, $H^{13}CHO$, and $HCH^{18}O$ were measured relative to DCDO to avoid overlapping spectral bands in the IR. Approximately 100 ppb of DCDO and 100 ppb of either HCHO, $H^{13}CHO$, or $HCH^{18}O$ were added to the chamber by heating paraformaldehyde polymer and flushing it into the chamber. SF_6 was added to monitor the leakage out of the chamber (see later) and actinic flux was measured by using a calibrated filter radiometer calibrated to the photolysis frequency of NO_2. The IR spectra were recorded every 10 min throughout the duration of the experiment by co-adding 500 interferograms obtained at a resolution of 1 cm^{-1}. Reactant and product concentrations were checked by spectral subtraction using calibrated reference spectra obtained at EUPHORE. For each experiment, the analysis of the gas mixture was started at least 30 min before exposing the mixture to sunlight to check for dark reactions. Each isotopic mixture was studied at least twice to ensure experimental reproducibility. The loss of formaldehyde in the dark was measured relative to that of SF_6. The results showed a negligible difference between the two losses, indicating that no heterogeneous and wall reactions of formaldehyde are taking place.

The HCHO isotopomers used were in the form of paraformaldehyde, $(CH_2O)_n$. DCDO (99 atom % D) was obtained as paraformaldehyde from Isotech, and $H^{13}CHO$ (99.8 atom % ^{13}C) was obtained from Aldrich as a formalin solution, which was freeze-dried to isolate the polymer. HCHO was obtained from Merck, and this chemical was also used to synthesize $HCH^{18}O$ by exchanging with $H_2{}^{18}O$ (95 atom % ^{18}O) from Campro Scientific. The $HCH^{18}O$ polymer thus obtained was determined by FTIR to be 90% pure, with 10% $HCH^{16}O$.

The relative rate method was used to extract the relative photolysis rates of the HCHO isotopomers. The decays of the concentrations of the species being photolyzed are measured simultaneously as a function of reaction time. Consider two simultaneous photolysis processes with the rates J_A and J_B:

$$\mathrm{A} + h\nu \xrightarrow{J_\mathrm{A}} \text{products}$$

$$\mathrm{B} + h\nu \xrightarrow{J_\mathrm{B}} \text{products} \tag{2}$$

Assuming that there are no loss processes other than these reactions and that there are no other processes producing the reactants, the following relation is valid:

$$\ln\left\{\frac{[\mathrm{A}]_0}{[\mathrm{A}]_t}\right\} = \frac{J_\mathrm{A}}{J_\mathrm{B}} \ln\left\{\frac{[\mathrm{B}]_0}{[\mathrm{B}]_t}\right\} \tag{3}$$

where $[A]_0$, $[A]_t$, $[B]_0$, and $[B]_t$ denote the concentrations of compounds A and B at times zero and t, respectively. A plot of

TABLE 1: Summary of Results[a] from Photolysis Experiments at EUPHORE in July 2003

	no corrections		k_{leak} correction		OH correction		all corrections		ϵ (‰)
experiment	$J_{rel} = J_x/J_y$	$\delta J_x/J_y$	$J_{rel} = J_y/J_y$	$\delta J_x/J_y$	$J_{rel} = J_x/J_y$	$\delta J_x/J_y$	$J_{rel} = J_x/J_y$	$\delta J_x/J_y$	$\epsilon = (J_{rel} - 1)$
July 15: DCDO/HCHO	0.483	0.004	0.589	0.002	0.486	0.003	0.590	0.002	
July 16: DCDO/HCHO	0.492	0.005	0.609	0.004	0.497	0.005	0.604	0.003	
July 17: DCDO/HCHO	0.470	0.003	0.606	0.004	0.478	0.003	0.600	0.002	
weighted average							**0.597**	**0.001**	**−403(2)**
July 18: DCDO/HCH^{18}O	0.560	0.012	0.650	0.012	0.562	0.010	0.655	0.010	
July 21: DCDO/HCH^{18}O	0.544	0.015	0.649	0.013	0.546	0.014	0.656	0.011	
weighted average							0.655	0.007	
relative to HCHO					HCH^{18}O/HCHO		**0.911**	**0.011**	**−89(11)**
July 22: DCDO/H^{13}CHO	0.542	0.008	0.674	0.005	0.543	0.007	0.666	0.004	
July 23: DCDO/H^{13}CHO	0.544	0.012	0.701	0.012	0.545	0.012	0.679	0.009	
weighted average							0.668	0.004	
relative to HCHO					H^{13}CHO/HCHO		**0.894**	**0.006**	**−106(6)**

[a] Errors are 1 σ from the fit. The results for each individual experiment are shown and the weighted mean for the corrected values, given by $\bar{X}_w = \sum W_i X_i / \sum W_i$, is shown. The results are shown uncorrected, corrected for leakage, corrected for reaction with OH, and corrected for both. The relative photolysis rate with respect to HCHO is calculated for H^{13}CHO and HCH^{18}O based on the J_{DCDO}/J_{HCHO} ratio.

$\ln([A]_0/[A]_t)$ vs $\ln([B]_0/[B]_t)$ will thus give the relative photolysis rate coefficient $\alpha = J_A/J_B$ as the slope, or in terms of the fractionation constant per mil, $\epsilon = (\alpha - 1) \times 1000$.

In the present case, however, three loss processes for the formaldehyde isotopomers in the chamber have to be taken into account: photolysis, reaction with OH, and leakage. Given that there are no formation processes of HCHO, the concentration of isotopomers A and B can be described by:

$$\frac{d[A]}{dt} = -(J_A + k_{leakage} + k_{OH}^{A}[OH])[A]$$

$$\frac{d[B]}{dt} = -(J_B + k_{leakage} + k_{OH}^{B}[OH])[B] \qquad (4)$$

where J_A and J_B are the photolysis rates, $k_{leakage}$ is the leakage rate, and k_{OH}^{A} and k_{OH}^{B} are the reaction rate coefficients for the OH reaction with A and B, respectively. Assuming that J_A and J_B have the same implicit time dependency the above equations may be solved to give the following relation:

$$\ln\frac{[A_0]}{[A_t]} + k_{leakage}t + \int_0^t k_{OH}[OH]\,dt = \frac{J_A}{J_B}\left(\ln\frac{[B_0]}{[B_t]} + k_{leakage}t + \int_0^t k_{OH}[OH]\,dt\right) \qquad (5)$$

The leakage rate of the chamber, $k_{leakage}$, was determined for each experiment by adding ca. 20 ppb SF_6 gas to the chamber and monitoring its removal by FTIR. The concentration of SF_6 was determined from the integrated intensity of its $\nu_3(F_{1u})$ band around 947.5 cm^{-1}, which overlaps the υ_6 band of DCDO. However, the absorption of the DCDO band is very weak, it contributes less than 1% to the integrated intensity of the SF_6 band, and it was therefore ignored in the derivation of the leakage rate:

$$\ln\{[SF_6]_0/[SF_6]_t\} = k_{leakage}t \qquad (6)$$

where $[SF_6]_0$ and $[SF_6]_t$ are the SF_6 concentrations at times zero and t, respectively. Typical values of $k_{leakage}$ in chamber A are $2-4 \times 10^{-5}$ s^{-1}.

The spectral features used in the analysis of the formaldehyde removal from the chamber were the C−H stretching bands in the 2670−2855 cm^{-1} region and the C−D stretching bands in the 2010−2190 cm^{-1} region. The compounds considered in each spectral region are given in Table 2. The spectral data needed in the fitting procedure were taken from the HITRAN database (HCHO, CO, CO_2, H_2O, NO, O_3); for DCDO, H^{13}CHO, and HCH^{18}O experimental high-resolution IR spectra were used. These spectra were recorded with a Bruker IFS 120 FTIR instrument at 0.01 cm^{-1} resolution in a 10 cm Pyrex gas cell equipped with CaF_2 windows. The partial pressures of formaldehyde isotopomers were in the range 6−10 mbar and the cell was filled to 1013 mbar with synthetic air (Air Liquide, dry technical air). The gas cell was passivated with ammonia before use to minimize the acid-catalyzed polymerization of the compound on the walls. A Ge on KBr beam splitter and 1800−4000 cm^{-1} band-pass filter were used in the interferometer and a globar (SiC_2) was used as the MIR light source. The detector was a liquid N_2 cooled InSb semiconductor detector and 128 scans were co-added to achieve an acceptable signal/noise ratio in the resultant spectra.

TABLE 2: Wavenumber Regions and Compounds Included in Fitting the Experimental Spectra[a]

HCHO isotopomer	spectral regions (cm^{-1})	compds included in spectral fitting
HCHO, H^{13}CHO, HCH^{18}O	2670−2855	HCHO, H^{13}CHO, HCH^{18}O, H_2O, O_3
DCDO	2010−2190	DCDO, CO, CO_2, H_2O, NO

[a] The experiments were carried out with three mixtures of HCHO isotopomers: (HCHO, DCDO), (DCDO, H^{13}CHO), and (DCDO, HCH^{18}O).

3. Results and Discussion

Figure 1 shows the overlap between the UV spectrum of HCHO and the actinic flux measured in the EUPHORE chamber on a typical day along with the quantum yields of channels 1a and 1b at atmospheric pressure.[34] As can be seen, the molecular channel dominates the photolysis at the wavelengths in the chamber. OH radicals are formed in the cell as hydrogen atoms from the formaldehyde photolysis react with O_2 to generate HO_2 and eventually H_2O_2, OH, and O_3. As there is always a small amount of NO_x present, depending in part on outside conditions, these reactions could generate enough OH that the OH + HCHO reaction would compete with photolysis. It is important to quantify the fraction of HCHO that reacts with OH as it is not only a loss process, it is also associated with a kinetic isotope effect, which could influence the result.[18] The reaction system was therefore examined in a FACSIMILE kinetic model based on the Master Chemical Mechanism and especially designed for the EUPHORE chamber to elucidate the extent of the

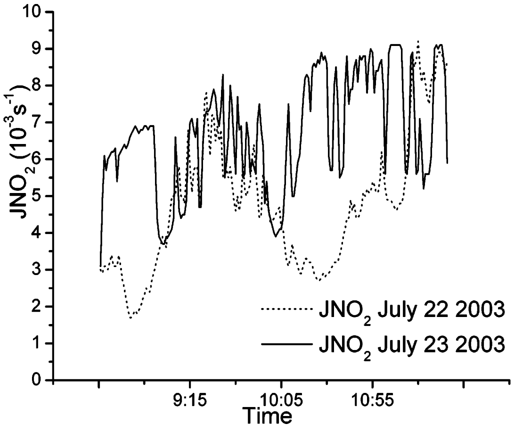

Figure 2. The $J(NO_2)$ measured in the chamber at EUPHORE for July 22 and 23, 2003. These values vary depending on cloud cover.

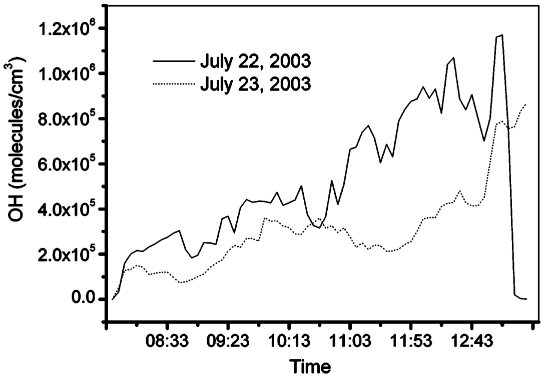

Figure 3. Facsimile simulation of the OH concentration in the EUPHORE chamber on July 22 and 23, 2003.[44] The model takes the photolysis rate of NO_2, temperature, and O_3 and NO_x concentrations as input and simulates the photochemistry based on the Master Chemical Mechanism.[45] The day-to-day variation is due to factors such as cloud cover, outside pollution, and wind conditions.

competing chemical reaction of HCHO with OH.[35] The model uses the temperature and photolysis rate of NO_2 recorded in the chamber each day, and the initial concentrations of NO_x, O_3, and reagents to simulate the OH concentration throughout the day for each day of experiments. The $J(NO_2)$ value is used to scale the photolysis rates of all species in the model to match the specific conditions of a given day. The measured $J(NO_2)$ values and calculated OH concentrations for two of the days in July 2003 are shown in Figures 2 and 3. The variation is quite considerable and is essentially due to cloud cover. These OH concentrations were used in the relative photolysis rate eq 5 to make the appropriate correction. The results before and after the correction are given in Table 1. The OH contribution is negligible, amounting to less than 1% of the total aldehyde removal in all cases. In a typical experiment about 70% of the light isotopomer was removed from the chamber. Of this, about 70% was removed by photolysis and about 30% by leakage. The correction for leakage is large, but as the leakage rate is constant throughout each experiment the correction does not greatly affect the accuracy of the result, as seen in Figure 4.

The concentrations of formaldehyde isotopomers as a function of photolysis time were extracted from the experimental infrared spectra by using a global FTIR nonlinear least-squares spectral fitting procedure, NLM4, developed by Griffith.[36] This method simulates the spectrum of the mixture of absorbing species from a set of initial concentrations and then varies the concentrations iteratively to minimize the residual between the measured and simulated spectrum. In the spectrum calculation, true absorption coefficients from the HITRAN database are used if available,[37] otherwise a high resolution measured spectrum can be used as a good approximation. The analysis of the FTIR spectra produced accurate values for the relative change in concentrations which were analyzed according to eq 5 using a weighted least-squares procedure that includes uncertainties in both reactant concentrations.[38] The relative photolysis rate plots are shown for three of the experiments in Figure 5.

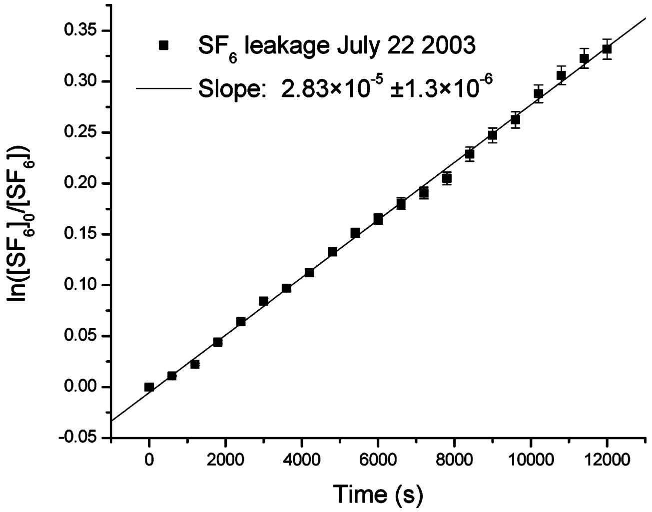

Figure 4. The integrated intensity of the SF_6 band relative to the initial intensity as a function of photolysis time. The slope corresponds to the loss rate for SF_6, which is used as a measure of the leakage from the chamber.

The results are summarized in Table 1 in the form $J_{DCDO}/J_{isotope}$ for each experiment. The weighted mean for each ratio is given, and for $H^{13}CHO$ and $HCH^{18}O$ the photolysis rate relative to HCHO is calculated from the J_{HCHO}/J_{DCDO} ratio. Wavelength-dependent isotopic fractionation factors have been modeled for N_2O using both time-dependent[39] and time-independent[40] methods. A useful approximation can be made using the "reflection principle"; isotopic substitution changes the shape and zero point energy of the vibrational wave function, leading to changes in the width and position of the absorption spectrum. While the reflection principle theory[40] is useful for predicting the isotope effect in direct photodissociation, it is not meant for systems such as formaldehyde where the absorption spectrum is highly structured and the excited state has a long lifetime. In such cases a reasonable understanding can be achieved using Franck−Condon integrals, considering the effect of isotopic substitution on the wave functions in the ground and excited states. Dynamic effects will also play a role.[41] The dynamic and spectroscopic effects are evident in the large isotope effect of 0.597 ± 0.001 seen in the J_{DCDO}/J_{HCHO} ratio. The relative reaction rates of DCDO and HCHO observed in the OH and Cl reactions of this isotopomer are likewise large, $k_{HCHO+OH}/k_{DCDO+OH} = 1.66(0.01)$ and $k_{HCHO+Cl}/k_{DCDO+Cl} = 1.31(0.01)$, respectively.[18] The photolysis rates of $H^{13}CHO$ and $HCH^{18}O$ are very similar, and within the present experimental error it is difficult to determine if the difference in the isotope effects is statistically significant. The isotope effect for both is of the order of 100‰ which is larger than the isotope effect associated with the reactions of these isotopomers with OH (20−30‰) and Cl (70−80‰).[18] The atmospheric fractionation factors emphasize the point that these isotope effects are considerable. In the case where all HCHO molecules are photolyzed or react with radicals, the resultant CO will have the same isotopic composition as the initial HCHO. If significant amounts are removed by dry

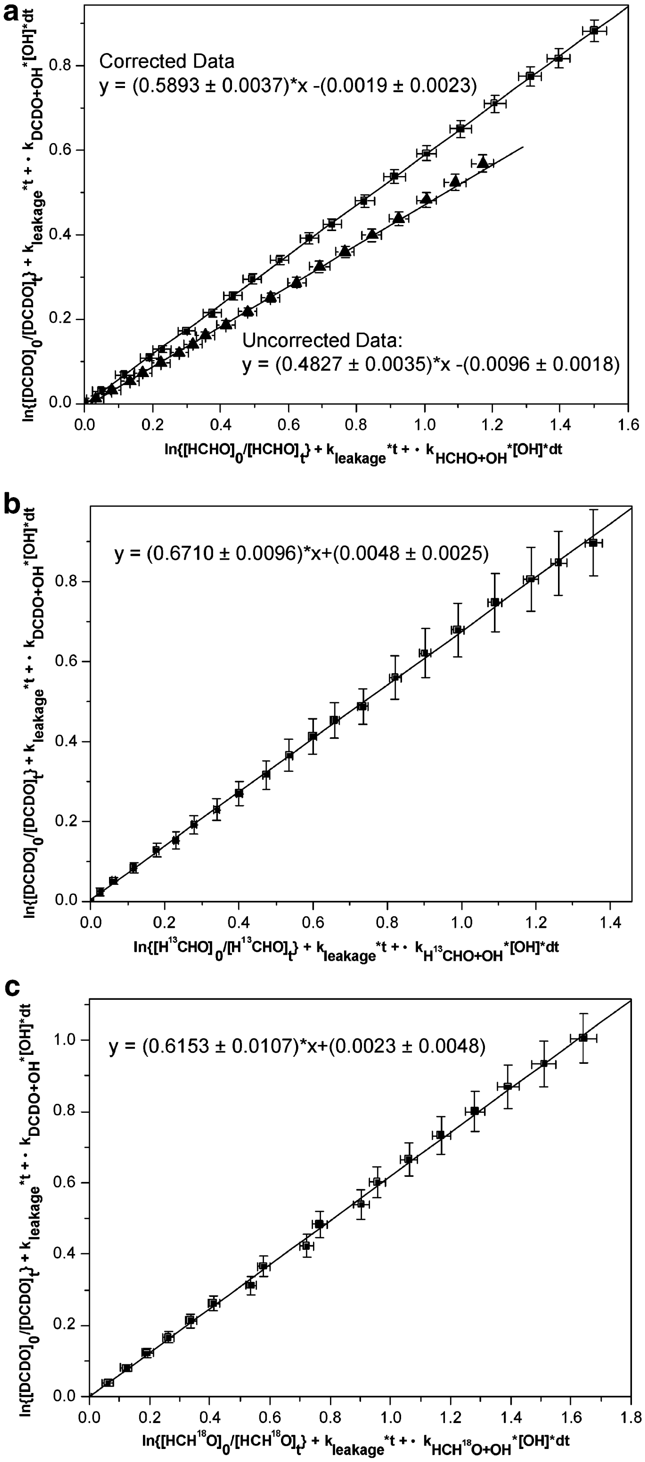

Figure 5. (a) Loss of HCHO and DCDO during actinic photolysis in the EUPHORE reactor on July 15, 2003. (b) Loss of $H^{13}CHO$ and DCDO during actinic photolysis in the EUPHORE reactor on July 22, 2003. (c) Loss of $HCH^{18}O$ and DCDO during actinic photolysis in the EUPHORE reactor on July 18, 2003. The slopes of the regression lines correspond to the relative photolysis rates = $J_{DCDO}/J_{isotope}$. The error bars assigned to each data point correspond to the 2σ errors of the spectral fit; see text for details. The intercepts are not statistically significant in any of the cases.

deposition and uptake into aerosols before it is photolyzed or reacts with radicals, the CO product will be enriched compared to the initial HCHO. Although the doubly substituted DCDO is rare in atmospheric samples, the deuterium fractionation factor of −403(2)‰ has implications for the deuterium enrichment in photochemically produced H_2.

4. Conclusion

The relative photolysis rates of HCHO, $H^{13}CHO$, and $HCH^{18}O$ with respect to DCDO were measured in natural sunlight conditions at the EUPHORE facility. The results show a large isotope effect in the J_{DCDO}/J_{HCHO} ratio with a mean value of 0.597 ± 0.001. Mechanistically this large effect most likely originates in the large change in the shape of the vibrational wave function and the zero point energy when substituting with deuterium. Although DCDO is not an atmospherically relevant isotopomer, this suggests that there may be a significant isotope effect in the photolysis of HCDO. HCDO is a very interesting isotopic species as its photolysis is the only in situ source of atmospheric HD. The atmospheric deuterium budget is uncertain and the H_2/HD enrichment could be an important tool for constraining it.[42,43]

The relative photolysis rates of $H^{13}CHO$ and $HCH^{18}O$ with respect to HCHO show that photolysis of these heavier isotopomers is about 10% slower than that for HCHO. The two ratios $J_{DCDO}/J_{H^{13}CHO} = 0.668 \pm 0.004$ and $J_{DCDO}/J_{HCH^{18}O} = 0.655 \pm 0.007$ are almost identical within experimental error and we cannot state at present if the difference in the isotope effects is statistically significant. The $J_{HCHO}/J_{H^{13}CHO}$ ratio is of interest when modeling the distribution of carbon isotopes throughout the oxidation chains of atmospheric hydrocarbons.

Acknowledgment. This work is part of the ACTION (Atmospheric Chemistry and Transport from Isotopic Analysis) project supported by the Norwegian Research Council. The authors thank the Danish Natural Science Research Council and the Nordic Network for Chemical Kinetics for their support. The authors are grateful to Claire Bloss and Roberto Sommariva at the University of Leeds for providing us with the customized FACSIMILE model.

References and Notes

(1) Anderson, L. G.; Lanning, J. A.; Barrel, R.; Miyagishima, J.; Jones, R. H.; Wolfe, P. *Atmos. Environ.* **1995**, *30*, 2113.

(2) Sumner, A. L.; Shepson, P. B.; Couch, T. L.; Thornberry, T.; Carroll, M. A.; Sillman, S.; Pippin, M.; Bertman, S.; Tan, D.; Faloona, I.; Brune, W.; Young, V.; Cooper, O.; Moody, J.; Stockwell, W. *J. Geophys. Res.* **2001**, *106*, 24387.

(3) Fried, A.; Lee, Y. N.; Frost, G.; Wert, B.; Henry, B.; Drummond, J. R.; Hübler, G.; Jobson, T. *J. Geophys. Res.* **2002**, *107*, 4039.

(4) Wang, Y.; Ridley, B.; Fried, A.; Cantrell, C.; Davis, D.; Chen, G.; Snow, J.; Heikes, B.; Talbot, R.; Dibb, J.; Flocke, F.; Weinheimer, A.; Blake, N.; Blake, D.; Shetter, R.; Lefer, B.; Atlas, E.; Coffey, M.; Walega, J.; Wert, B. *J. Geophys. Res.* **2003**, *108*, 8358.

(5) Smith, G. D.; Molina, L. T.; Molina, M. J. *J. Phys. Chem. A* **2002**, *106*, 1233.

(6) Seinfeld, J. H.; Pandis, S. N. *Atmospheric Chemistry and Physics*: *From Air Pollution to Climate Change*; John Wiley & Sons: New York, 1998.

(7) Allan, W.; Lowe, D. C.; Cainey, J. M. *Geophys. Res. Lett.* **2001**, *28*, 3239.

(8) Atkinson, R.; Baulch, D. L.; Cox, R. A.; Crowley, J. N.; Hampson, R. F., Jr.; Kerr, J. A.; Rossi, M. J.; Troe, J. *Summ. Evaluated Kinetic Photochem. Data Atmos. Chem.* **2001**.

(9) Lowe, D. C.; Schmidt, U. *J. Geophys. Res.* **1983**, *88*, 10884.

(10) Barrie, L. A.; Bottenheim, J. W.; Schnell, R. C.; Crutzen, P. J.; Rasmussen, R. A. *Nature* **1988**, *334*, 138.

(11) Shepson, P. B.; Sirju, A. P.; Hopper, J. F.; Barrie, L. A.; Young, V.; Niki, H.; Dryfhout, H. *J. Geophys. Res.* **1996**, *101*, 21081.

(12) Pope, F. D.; Smith, C. A.; Davis, P. R.; Shallcross, D. E.; Ashford, M. N. R.; Orr-Ewing, A. J. *Faraday Discuss.* **2005**, *130*, 1.

(13) Rogers, J. D. *J. Phys. Chem.* **1990**, *94*, 4011.

(14) Chuang, M.; Foltz, M. F.; Moore, C. B. *J. Chem. Phys.* **1987**, *87*, 3855.

(15) Wagner, V.; von Glasow, R.; Fischer, H.; Crutzen, P. J. *J. Geophys. Res.* **2002**, *107*, 1.

(16) Brenninkmeijer, C. A. M.; Jannsen, C.; Kaiser, J.; Röckmann, T.; Rhee, T. S.; Assonov, S. S. *Chem. Rev.* **2003**, *103*, 5125.

(17) Rahn, T.; Eiler, J. M.; Boering, K. A.; Wennberg, P. O.; McCarthy, M. C.; Tyler, S.; Schauffler, S.; Donnell, S.; Atlas, E. *Nature* **2003**, *424*, 918.

(18) Feilberg, K. L.; Johnson, M. S.; Nielsen, C. J. *J. Phys. Chem. A* **2004**, *108*, 7393.

(19) D'Anna, B.; Bakken, V.; Beukes, J. A.; Nielsen, C. J.; Brudnik, K.; Jodkowski, J. T. *Phys. Chem. Chem. Phys.* **2003**, *5*, 1790.

(20) Beukes, J. A.; D'Anna, B.; Bakken, V.; Nielsen, C. J. *Phys. Chem. Chem. Phys.* **2000**, *2*, 4049.

(21) Beukes, J. A.; D'Anna, B.; Nielsen, C. J. *Asian Chem. Lett.* **2000**, *4*, 145.

(22) Marling, J. B. *High single-step enrichment of rare stable isotopes by ion laser formaldehyde photo-predissociation*, Report; Lawrence Livermore Lab., University California: Livermore, CA, 1976.

(23) Marling, J. *J. Chem. Phys.* **1977**, *66*, 4200.

(24) Marling, J. B. *Chem. Phys. Lett.* **1975**, *34*, 84.

(25) Marling, J. B. patent 76-697000, 40295594, 1976.

(26) Marling, J. B. patent 76-734840, 40295586, 1976.

(27) Marling, J. B. *Opt. Commun.* **1976**, *18*, 36.

(28) Leung, F.-Y. T.; Colussi, A. J.; Hoffmann, M. R.; Toon, G. C. *Geophys. Res. Lett.*, **2002**, *29*, 10.1029.

(29) von Hessberg, P.; Kaiser, J.; Enghoff, M. B.; McLinden, C. A.; Sorensen, S. L.; Röckmann, T.; Johnson, M. S. *Atmos. Chem. Phys.* **2004**, *4*, 1237.

(30) Farquhar, J.; Bao, H.; Thiemens, M. H. *Science* **2000**, *289*, 756.

(31) Battacharya, S. K.; Savarino, J.; Thiemens, M. H. *Geophys. Res. Lett.* **2000**, *27*, 1459.

(32) Farquhar, J.; Savarino, J.; Airieau, S.; Thiemens, M. H. *J. Geophys. Res.* **2001**, *106*, 32829.

(33) Becker, K. H. *The European Photoreactor EUPHORE, Design and Technical Development of the European Photoreactor and First Experimental Results*, Final Report of the EC-Project Contract EV5V-CT92-0059, 1996.

(34) DeMore, W. B.; Sander, S. P.; Golden, D. M.; Hampson, R. F.; Kurylo, M. J.; Howard, C. J.; Kolb, C. E.; Molina, M. J. *Chemical kinetics and photochemical data for use in stratospheric modeling*; Evaluation number 14, JPL Publication 02-25, 2003.

(35) Bloss, C.; Wagner V.; Bonzanini, A.; Jenkin, M. E.; Wirtz, K.; Martin-Reviejo, M.; Pilling, M. J. *Atmos. Chem. Phys. Discuss.* **2004**, *4*, 5683.

(36) Griffith, D. W. T. *Appl. Spectrosc.* **1996**, *50*, 59.

(37) Rothman, L. S.; Barbe, A.; Chris Benner, D.; Brown, L. R.; Camy-Peyret, C.; Carleer, M. R.; Chance, K.; Clerbaux, C.; Dana, V.; Devi, V. M. *J. Quant. Spectrosc. Radiat. Transfer* **2003**, *82*, 5.

(38) York, D. *Can. J. Phys.* **1966**, *44*, 1079.

(39) Nanbu, S.; Johnson, M. S. *J. Phys. Chem. A* **2004**, *108*, 8905.

(40) Blake, G. A.; Liang, M.-C.; Morgan, C. G.; Yung, Y. L. *Geophys. Res. Lett.* **2003**, *30*, 1656.

(41) Bamford, D. J.; Filseth, S. V.; Folzt, M. F.; Hepburn, J. W.; Moore, C. B. *J. Chem. Phys.* **1985**, *82*, 3032.

(42) Prather, M. J. *Science* **2003**, *302*, 581.

(43) McCarthy, M. C.; Boering, K. A.; Rice, A. L.; Tyler, S. C.; Connell, P.; Atlas, E. *J. Geophys. Res.* **2003**, *108*, 4461.

(44) *FACSIMILE* for Windows, Version 4.0.30; MCPA Software Ltd., 2004.

(45) Jenkin, M. E.; Saunders, S. M.; Wagner, V.; Pilling, M. J. *Atmos. Chem. Phys.* **2003**, *3*, 181.